$^{51}V(n,\gamma)$ reaction in the keV incident neutron energy range*

R. R. Winters
Denison University, Granville, Ohio 43203

R. L. Macklin and J. Halperin
Oak Ridge National Laboratory, Oak Ridge, Tennessee 37830
(Received 28 November 1977; revised manuscript received 19 June 1978)

The $^{51}V(n,\gamma)$ cross section has been measured at the electron linear accelerator capture facility. This very high resolution experiment has allowed the extraction of capture areas for some 139 resonances for incident neutron energies 2.5-215 keV. The capture data combined with spin and parity assignments and a few neutron widths from the literature provide full sets $(E_\gamma, \Gamma_\gamma, \Gamma_n)$ of the resonance parameters for 45 s-wave resonances. Analysis of these parameters has yielded values for the s-wave strength function $\langle S\rangle^{l=0}_{J=3} = (8.3^{+4.0}_{-2.5})\times 10^{-4}$ and $\langle S\rangle^{l=0}_{J=4} = (7.0^{+3.8}_{-2.2})\times 10^{-4}$ (10–90% confidence interval). The mean level spacing found for the $J^\pi = 4^-$ levels is $\langle D\rangle^{l=0}_{J=4} = (9.8^{+0.8}_{-0.5})$ keV. The $J^\pi = 3^-$ mean level spacing $\langle D\rangle^{l=0}_{J=3} = (7.8^{+0.5}_{-1.7})$ keV derived from this work is less well determined than that for the 4^- levels because of an apparent change in mean level spacing near 100 keV. This effect is probably due to levels with widths too small compared to the resolution width for parity to be determined and/or to levels not seen in this work. The s-wave total radiation widths are large and fluctuate widely; $\langle\Gamma_\gamma\rangle^{l=0}_{J=3} = 1467 \pm 183$ meV and $\langle\Gamma_\gamma\rangle^{l=0}_{J=4} = 1629 \pm 352$ meV. The variance of these distributions are consistent with χ^2 distributions of 5 degrees of freedom for the 3^- resonances and 2 degrees of freedom for the 4^- resonances. The reduced neutron widths and the total radiative widths for the 4^- s-wave resonances exhibit strong correlation ($\rho = 0.93$, significant at $> 99.9\%$ confidence level), but the 3^- s waves are less significantly correlated ($\rho = 0.42$ significant at the 96% confidence level). The contribution of these resonances to the thermal capture cross section is determined to be 3.95 b, approximately 80% of the measured thermal value. The capture resonance integral derived from this work is in good agreement with the published value. The 30 keV Maxwellian averaged cross section (41 ± 3) mb is of interest in stellar nucleosynthesis.

NUCLEAR REACTIONS $^{51}V(n,\gamma)$, $E = 2.6$–215 keV; measured $\sigma_\gamma(E)$; deduced $(^{51}V+n)$ resonance parameters, S_0, D, Γ_γ for $J=3^-$, 4^- separately, $(\Gamma_n^0 \Gamma_\gamma)$ correlation coefficients significant for $J=4^-$, resonance integral, stellar average cross sections. 25.40.Lw

INTRODUCTION

Vanadium may be of importance as a structural material in fusion energy conversion processes. In particular, a study by Steiner[1] shows that vanadium offers significant advantages over niobium for use in fusion reactor blankets. Steiner finds that vanadium compared to niobium has superior tritium breeding characteristics, produces less nuclear heating in the first blanket wall, and results in significantly lower after-shutdown biological hazard. The validity of such comparisons depends on the cross sections used in the calculations. However, both the BNL-325[2] compilation and the even more recent ANL/NDM-24[3] evaluation of the $V(n,\gamma)$ cross section indicate large discrepancies (~50%) among the relatively few published measurements. Such uncertainties might be reduced with better estimates of the $^{51}V+n$ resonance parameters in the kilovolt incident neutron energy range.

In addition to its importance in fusion power operation, vanadium is of current interest for nuclear models. McGrory[4] and Horie and Ogawa[5] have shown that the relatively simple model of ^{52}V as a ^{48}Ca core coupled to single-particle configurations such as

$$[\pi f^3{}_{7/2}\nu(2p_{1/2,3/2} \text{ or } f_{5/2})]$$

is at least approximately valid. Should this simple structure persist into the unbound region, then, as pointed out by Bird[6] *et al.*, the capture process $^{51}V(n,\gamma)$ might be strongly dominated by single-particle, particularly valency, effects. Testing of such simple single-particle models requires an extensive set of resonance parameters.

Recent neutron transmission studies by Garg[7] and the previous excellent work by Morgenstern *et al.*,[8] by Stieglitz *et al.*,[9] and by other workers (see BNL-325[10]) have provided a sizeable body of neutron widths, spins and parity assignments for $^{51}V+n$ resonances over the (1.0–200) keV energy region. However, radiative widths for only 13 $^{51}V+n$ resonances are reported in BNL-325.[10] Capture areas are listed for an additional eight resonances and one of these (at 18 keV) is seen to

 © 1978 The American Physical Society

be a doublet with our energy resolution. The present measurement of the $V(n,\gamma)$ cross section and the resulting resonance parameters complement and extend the set of parameters previously available both for the cross section evaluation and for nuclear structure studies.

EXPERIMENT

A 20.41 gm natural vanadium (99.76% ^{51}V) rectangular (2.625 cm × 5.090 cm) sample of thickness 0.0177 nuclei/b was used for the capture cross section measurements. The sample was inserted in a neutron beam of the Oak Ridge Electron Linear Accelerator (ORELA) at the 40.121 m experimental station on flight path 7. The electron burst width was 5 ns full width at half maximum (FWHM), resulting in a neutron energy resolution of $\Delta E/E = \frac{1}{700}$ to $\frac{1}{500}$ FWHM over the range 2.5 keV $\leq E \leq 200$ keV. The neutron energy was derived from time-of-flight and the energy resolution was dominated by the neutron moderation time. The resolution profile is well described by a Gaussian shape, part of which (30%) is further convoluted with an exponential tail with a decay time of 70% of the FWHM of the Gaussian. The resolution function was checked by fitting a few selected very narrow resonances. Figure 1 shows a closely spaced 40 eV centroid to centroid doublet (reported in BNL-325[10] as a single p-wave resonance) at 18.04 keV which is clearly resolved and illustrates the good resolution of the capture experiment.

Prompt capture γ rays were detected using two C_6F_6-based liquid scintillators situated on either side of the sample perpendicular to the direction of the neutron beam. The pulse heights resulting from detection of the capture γ rays were used to weight the time-of-flight events so as to make the detector efficiency independent of the details of the nuclear decay γ cascade which can vary greatly from resonance to resonance. With this weighting, the detector's efficiency is a function of the total energy (binding plus kinetic) released in the decay. These total energy detectors (TED) are described along with the experimental arrangement in a paper by Macklin and Allen.[11] The neutron spectrum was monitored with a 0.05 cm $^6Li(n,\alpha)$ glass scintillator.[12] The ratio of the efficiencies of the TED's and the neutron monitor was determined to ~2% accuracy by saturating the 4.9 eV resonance in gold using a thin (0.005 cm) gold foil in the sample position.

The data were corrected for all known backgrounds leaving a residual background of ≈ 10 mb at 2.5 keV dropping to ≲1 mb at 200 keV. A correction calculated to be 7.4% was made to the data to compensate for the energy loss of γ rays in the sample. An additional "background" is that due to neutrons scattered at a resonance ($E_\lambda, \Gamma_n, \Gamma_\gamma$) into the environment of the detectors, ultimately being captured and the resulting γ detected. This

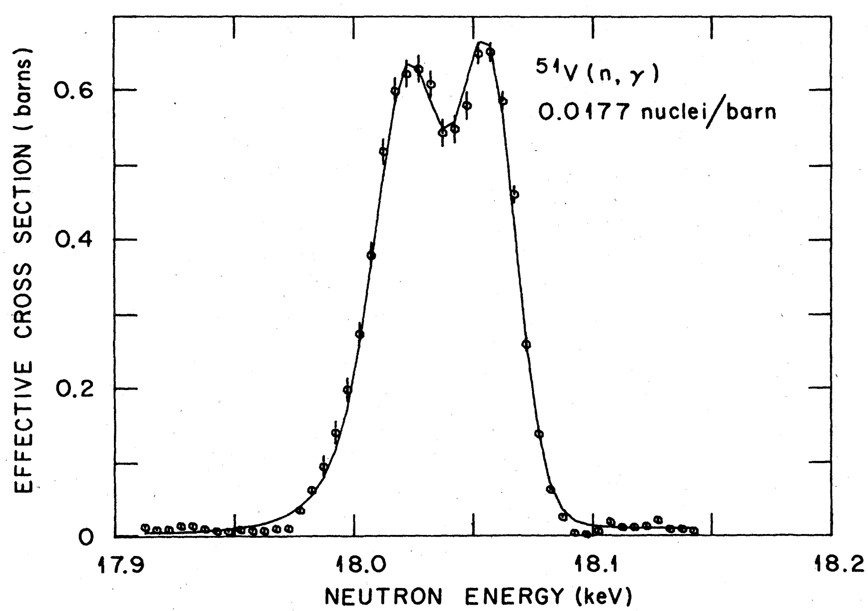

FIG. 1. A close doublet (previously reported as a single p-wave resonance) at 18 keV in the $^{51}V(n,\gamma)$ cross section. The solid curve is the Breit-Wigner single-level fit to the data obtained using the code LSFIT.

prompt background results in an enhancement of the observed radiative width Γ_γ^{obs} given by

$$\Gamma_\gamma^{obs} = \Gamma_\gamma + K(E,A)\Gamma_n , \quad (1)$$

where the scattered-neutron sensitivity $K(E,A)$ is a function of the ORELA capture facility geometry, the neutron energy, and the mass of the scattering nucleus. Values used for this troublesome background have been included in all tables of resonance parameters. As discussed by Allen *et al.*,[13] the parametrization of $K(E,A)$ is considered accurate to within a 20% uncertainty. An experimental determination independent of the parametrization given in Ref. 13 has been reported by Allen and Macklin.[14] Using the 254 keV resonance in ^{7}Li$+n$, these workers find $K=(0.13\pm0.04)\times10^{-3}$, a value which compares very well with the value $K=(0.11\pm0.02)\times10^{-3}$ from Ref. 13. The erros reported for capture areas and radiative widths requiring a non-negligible correction for scattered neutron sensitivity include the 20% uncertainty in $K(E)$.

ANALYSIS

Two curve fitting computer codes were used to analyze the observed peaks in the capture cross section over the incident neutron energy range 2.5 keV–215 keV. Nearly all of the analysis was performed using a nonlinear least squares code ORGLS2 originally developed by Busing and Levy and modified as LSFIT for capture cross section analysis by Macklin.[15] LSFIT fits each peak with the Doppler and resolution-broadened Breit-Wigner single-level resonance form

$$\sigma_\gamma(E) = \pi ƛ(E) ƛ(E_R)\frac{g\Gamma_n(E_R)\Gamma_\gamma}{(E-E_R)^2+(\Gamma(E)/2)^2} \quad (2)$$

[where $\Gamma(E)=(ƛ(E_R)/ƛ(E))\Gamma_n(E_R)+\Gamma_\gamma$] plus a background term which has an $E^{-1/2}$ dependence. LSFIT also treats multiple scattering in the sample following neutrons through the fourth interaction. The treatment of multiple scattering has been shown to yield the same results as more conventional Monte Carlo calculations when the multiple scattering contributes $\lesssim 50\%$ of the observed capture yield.

The three wide s-wave resonances at 4.148, 6.797, and 11.62 keV were fitted with the Monte Carlo code TACASI originally developed by Fröhner[16] and modified to handle ORELA capture data by Spencer.[17] Figure 2 shows the fit to the 11.32 keV resonance data using this Monte Carlo code.

Tables I–IV list the resonance parameters resulting from the analysis of some 139 resonances. Note that in a substantial number of cases the ORELA resolution is good enough to allow the extraction of both the neutron width and the radiative width if the spin of the resonance is known. In those cases in which the resonance is narrow compared to the ORELA resolution, we have used the neutron widths and spin assignments as given in BNL-325 or, above 153 keV, as reported by

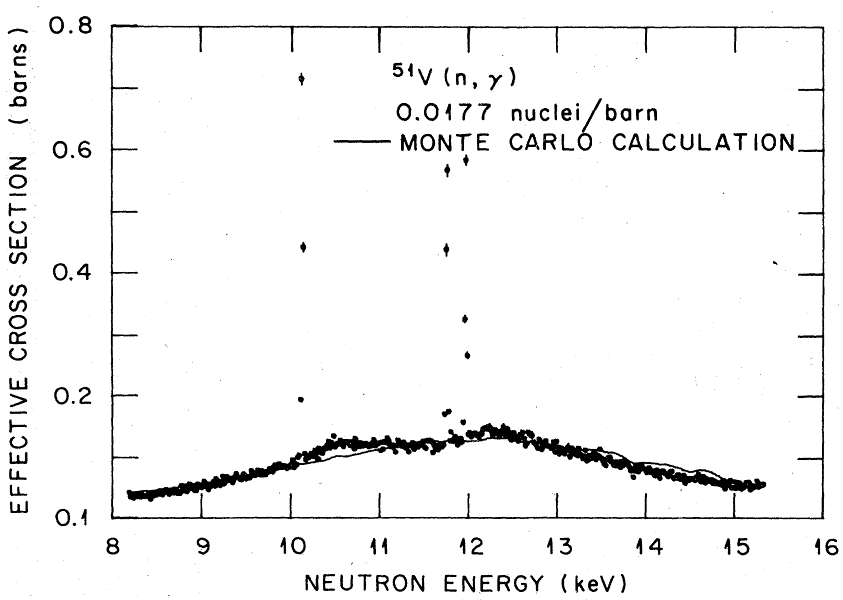

FIG. 2. The broad s-wave resonance near 12 keV in the ^{51}V(n,γ) cross section. The solid curve is the fit to the data obtained using the Monte Carlo code TASCAI. The three narrow resonances were not included in the fit shown here.

TABLE I. $^{51}V + n$ resonance parameters 4–45 keV.

This work E_γ (keV)	This work $g\Gamma_n\Gamma_\gamma/(\Gamma_n+\Gamma_\gamma)$ (meV)	This work $g\Gamma_n$ (eV)	BNL−325 $g\Gamma_n$ (eV)	BNL−325 J	BNL−325 ℓ	This work Γ_γ (meV)	BNL−325 Γ_γ (meV)	$K(E)\times10^3$	This work $g\Gamma_n^\ell$ (eV)
4.148 ± 0.006	1096 ± 56		282 ± 3	4	0	1100 ± 100	1320 ± 200	0.21	4.35 [d]
4.385	111 ± 2				1				
6.797	1794^{+262}_{-44}		560 ± 6	3	0	1800^{+600}_{-100}	2450 ± 360	0.32	6.56 [d]
7.03 ± 0.01	36 ± 1	0.040 ± 0.002			1	535 [c]			0.050
10.13	88 ± 2				1				
11.62	1050 ± 131		2125 ± 25	3	0	2400 ± 300	1870 ± 370	0.21	19.58 [d]
11.76 ± 0.02	56 ± 2	0.069 ± 0.003			1	535 [c]			0.040
11.97	54 ± 2	0.066 ± 0.002			1	535 [c]			0.037
15.70 ± 0.02	172 ± 9				1				
16.21	490 ± 42	182 ± 19	194 ± 13	4	0	871 ± 75	1500 ± 500	0.21	1.43
16.90	283 ± 33	87 ± 14	115 ± 10	3	0	648 ± 75		0.21	0.669
18.02	122 ± 4 [a]								
18.06	119 ± 3 [a]								
20.75	233 ± 6				1				
21.21	28 ± 2								
21.71	403 ± 17	216 ± 12	317 ± 23	3	0	920 ± 39	1500 ± 180	0.21	1.77
24.23	122 ± 3				1				
28.84 ± 0.04	61 ± 3				1				
29.54	515 ± 17	94 ± 3	75 ± 10	4	0	915 ± 30	500 ± 60	0.41	0.547
30.03	173 ± 6		1.5 ± 0.5	(3)	1	395 ± 14	530 ± 150		0.217 [d]
32.29	65 ± 3				1				
33.55	157 ± 14	11 ± 3	11.4 [b] ± 2.2	3 [b]	0 [b]	538 ± 53	500 ± 80		0.060
37.49	391 ± 13	12 ± 1	13 ± 3	(4)	1	695 ± 23	550 ± 100		1.3
39.44	892 ± 26	249 ± 8	235 ± 18	3	0	2040 ± 60	980 ± 120	0.34	1.25
39.45	107 ± 14								
41.02 ± 0.06	804 ± 19		3.0 ± 1.0	(5)	1	1177 ± 28	1200 ± 300		0.28
42.36	270 ± 11	22 ± 5	22 [b] ± 3	4 [b]	0 [b]	630 ± 26	570 ± 110		0.11
44.70	114 ± 5		11 [b] ± 2	3 [b]	0 [b]	376 ± 16			0.05 [d]

[a] Previous work identified this doublet as a single p wave.
[b] Value taken from Garg (1977).
[c] Assumed radiative width (capture area measures $g\Gamma_n$).
[d] Calculated using $g\Gamma_n$ from BNL−325.

TABLE II. $^{51}V + n$ resonance parameters 45–105 keV.

This work E_γ (keV)	This work $g\Gamma_n\Gamma_\gamma/(\Gamma_n+\Gamma_\gamma)$ (meV)	This work $g\Gamma_n$ (eV)	BNL–325 $g\Gamma_n$ (eV)	BNL–325 J	BNL–325 ℓ	This work Γ_γ (meV)	$K(E)\times 10^3$	This work $g\Gamma_n^\ell$ (eV)
45.90	204 ± 7		5 ± 2	2^c	1	653 ± 23		1.17
48.06	235 ± 9	56 ± 3	65 ± 10	4	0	418 ± 16		0.25
48.64	425 ± 15		7.5 ± 2.5					
49.45	836 ± 24	249 ± 8	245 ± 18	3	0	1912 ± 55	0.29	1.12
50.61 ± 0.08	103 ± 5							
51.89	213 ± 20	63 ± 8	49.5 ± 4.0	4	0	378 ± 35		0.27
52.79	887 ± 32	383 ± 15	408 ± 30	3	0	2027 ± 72	0.29	1.67
55.18	112 ± 9							
61.11	25 ± 4	0.027 ± 0.005		4^d		535^e		
63.01	1549 ± 155	1440 ± 340	1650 ± 150	3	0	3540 ± 355	0.21	5.74
64.94	149 ± 11							
67.11	105 ± 7							
68.54	100 ± 8							
68.50	1766 ± 73	2100 ± 97	2654 ± 78	4	0	3605 ± 208	0.21	8.02
70.86 ± 0.12	169 ± 11							
70.96	105 ± 8							
72.10	83 ± 8							
72.74	147 ± 10							
73.52	384 ± 24		8.3^b ± 1.8	3^b	0	878 ± 55		0.031^b
74.17	153 ± 10							
76.73	192 ± 8							
76.89	104 ± 6							
78.80	149 ± 8		7.3^b ± 1.7	4^b	0^b	486 ± 26	0.21	0.036^b
80.59 ± 0.14	226 ± 9							
82.31	511 ± 90	774 ± 87	700 ± 50	4	0	910 ± 160	0.21	2.70
84.04	64 ± 7	0.082 ± 0.011		4^d		535^e		
83.7^a	<50							
86.10	213 ± 13							
87.00	289 ± 5							
87.29	1012 ± 84	1150 ± 90	1640 ± 120	4	0	1800 ± 150	0.20	3.89
89.94 ± 0.17	221 ± 13							
91.55	67 ± 10	0.085 ± 0.017				535^e		
93.08	224 ± 12	40 ± 5	38^b ± 7	3^b	0^b	516 ± 29		0.13
94.72	127 ± 10							
95.02	445 ± 24	37 ± 4	41^b ± 8	4^b	0^b	791 ± 43	0.18	0.12
95.70	227 ± 14		25 ± 8	4^d		499 ± 26		
97.12	163 ± 11		12 ± 6	3^d		372 ± 36		
98.41	640 ± 35		25 ± 8	4^d		1230 ± 72		
101.70 ± 0.20	238 ± 11							
103.70	154 ± 11		12 ± 5	3^d		352 ± 25		

[a] Morgenstern (1969) reports this resonance.
[b] Taken from Garg (1977).
[c] Tentative assignment BNL–325.
[d] Tentative assignment from this work.
[e] Radiative width fixed (capture area measures $g\Gamma_n$).

Garg.[7] In general the neutron widths extracted from the capture data agree well with the values found in those references. However, there are a few exceptions which will be discussed in the following sections.

In the range 215–300 keV there are 22 well-defined peaks, most with widths dominated by the ORELA energy resolution ($\Delta E = 0.38$ keV at 200 keV). These may represent multiple resonances and were not analyzed, although in Table V their energies are listed.

2.5–45 keV

This region (see Fig. 3 and Table I) is dominated by the 4.148, 6.797, and 11.62 keV broad, overlapping, s-wave resonances. Multiple scattering within the sample accounted for ~75% of the ob-

TABLE III. $^{51}V+n$ resonance parameters 105–131 keV.

This work E_γ (keV)	Morgenstern[8] E_γ (keV)	Garg[7] E_γ (keV)	This work $g\Gamma_n\Gamma_\gamma/(\Gamma_n+\Gamma_\gamma)$ (meV)	This work $g\Gamma_n$ (eV)	Morgenstern $g\Gamma_n$ (eV)	Garg $g\Gamma_n$ (eV)	Garg J^π	This work Γ_γ (meV)	$K(E)\times 10^3$	This work $g\Gamma_n^\ell$ (eV)
106.93 ± 0.20			262 ± 11	<50						
110.32	110.1	110.7	636 ± 46	376 ± 43	140 ± 30	381 ± 35	3^-	1455 ± 106	0.18	1.13
112.7[a]		112.7	<167[c]	450[a]		450 ± 281	4^-	<297[c]	0.18	1.34[a]
112.94			252 ± 28	94 ± 19			3[d]	576 ± 64		
113.64			271 ± 24	<50						
113.88			151 ± 23	<50						
114.40 ± 0.21	114.0	114.5	394 ± 80	100 ± 30	35 ± 15	525 ± 131	3^-	901 ± 183		0.296
116.1[a]	116.0	116.1	<197[c]	562[a]	2250 ± 400	562 ± 281	4^-	<350[c]	0.17	1.65[a]
116.15			172 ± 13	<50						
116.65			207 ± 13	<50						
117.5[b]					8440 ± 1200					
118.00	118.1		39 ± 10	<50	90 ± 20					
118.40			171 ± 16	<50						
118.62			101 ± 19	<50						
118.7[b]		118.7	3092 ± 357	4500[a]		4500 ± 1125	4^-	5498 ± 634	0.15	13.06[a]
119.25			104 ± 12	<50						
119.69			70 ± 11	<50						
121.43 ± 0.23			135 ± 14	<50						
121.6[a]		121.6	407 ± 269	2625[a]		2625 ± 875	3^-	931 ± 616	0.15	7.53[a]
122.55			131 ± 26							
126.0[a]		126.0	<90[c]	281[a]		281 ± 112	4^-	<159[c]	0.14	0.792[a]
127.0[a]		127.0	<100[c]	219[a]		219 ± 90	3^-	<229[c]	0.14	0.615[a]
129.17	128.7	129.4	428 ± 10	54 ± 5	35 ± 15	478 ± 169	4[d]	767 ± 80		
130.70 ± 0.25	130.3		725 ± 25	64 ± 5	50 ± 15		4[d]	1253 ± 160		

[a]From Garg.
[b]See discussion in text.
[c]Upper limit is observed value not corrected for $k(E)$.
[d]Tentative assignment (this work).

TABLE IV. $^{51}V + n$ resonance parameters 131–215 keV.

This work E_γ (keV)	Garg[7] E_γ (keV)	This work $g\Gamma_n\Gamma_\gamma/(\Gamma_n+\Gamma_\gamma)$ (meV)	This work $g\Gamma_n$ (eV)	Garg $g\Gamma_n$ (eV)	Garg J^π	This work Γ_γ (meV)	$K(E)$ $\times 10^3$	This work $g\Gamma_n^\ell$ (eV)
132.88 ± 0.27		328 ± 34	69 ± 10					
133.18		219 ± 26	<50					
134.98	134.7	1380 ± 121	2050 ± 220	2554 ± 225	4^-	2452 ± 215	0.14	5.58
135.05		263 ± 32	93 ± 19					
138.28		390 ± 21	<50					
140.60	140.6	1183 ± 118	1090 ± 110	1562 ± 131	3^-	2700 ± 270	0.14	2.91
143.28		953 ± 44	100 ± 20					
145.13	145.5	326 ± 37	368 ± 48	1181 ± 131	3^-	745 ± 85	0.15	1.01
147.42		101 ± 14	<50					
148.34		183 ± 20	65 ± 25					
151.02 ± 0.30		253 ± 28	<50					
151.54		794 ± 45	<50					
152.60		410 ± 219	502 ± 230					
152.72	152.5	424 ± 262	1760 ± 450	1881 ± 131	3^-	970 ± 400	0.15	4.50
155.48		117 ± 21	<50					
157.21		176 ± 27	<50					
159.60 ± 0.40		1159 ± 167	1660 ± 250	5625 ± 844	4^-	2060 ± 296	0.15	4.16
161.45		692 ± 77	467 ± 74					
162.95		314 ± 24	< 50					
164.25		440 ± 59	459 ± 94					
166.36		184 ± 23	<50					
166.7[a]	166.7	1403 ± 215	3369[a]	3369 ± 219	3^-	3208 ± 491	0.15	8.25[a]
168.20		107 ± 25	<50					
169.45		121 ± 25	<50					
170.9 ± 0.4		405 ± 29	122 ± 13					
172.9	172.0	810 ± 77	1137[a]	1137 ± 88	3^-	1850 ± 175	0.15	2.74[a]
174.6		214 ± 26						
175.8		443 ± 31						
176.5		335 ± 35						
	177	<160[c]	1744[a]	1744 ± 169	4^-	<284[c]	0.14	4.15[a]
179.2		149 ± 40						
179.3	179	1103 ± 194	1444[a]	1444 ± 131	3^-	2521 ± 443	0.14	3.41[a]
181.5[b]		482 ± 37						
183.0[a]	183	1472 ± 198	2925[a]	2925 ± 225	4^-	2617 ± 352	0.14	6.84[a]
183.7		120 ± 36	62 ± 20					
187.2[b]		514 ± 76						
187.5		340 ± 65						
188.0[a]	188	1879 ± 218	4331[a]	4331 ± 159	4^-	3340 ± 388	0.13	9.99[a]
188.9		100 ± 62	148 ± 60					
191.7		133 ± 24						
193.8	194	437 ± 87	736[a] ± 190	656 ± 219	3^-	1000 ± 198	0.12	1.67[a]
195.9		146 ± 27	77 ± 17					
197.7		178 ± 32						
199.5[b]		592 ± 51						
201.0	200	2950 ± 345	4390 ± 590	4162 ± 394	4^-	5250 ± 609	0.12	9.79[a]
204.9		180 ± 37						
207.3		215 ± 33	139 ± 32		(3)[d]	491 ± 75		
210.5	211	794 ± 143	1090[a] ± 210	525 ± 88	3^-	1814 ± 327	0.12	2.38[a]
212.2		210 ± 37	186 ± 42		(3^+)[d]	480 ± 85		1.78

[a] Garg[7].
[b] Possible multiplet.
[c] Upper limit is observed value not corrected for $K(E)$.
[d] Tentative assignment.

TABLE V. Centroid energies of peaks above 215 keV.

E_λ (keV)	E_λ (keV)	E_λ (keV)	E_λ (keV)	E_λ (keV)
216	229[a]	240	260	290
217	232[a]	242	263	299
221	236[a]	245	272	
224	237	248	281	
226	238	258	285	

[a] Peak width broad compared to the ORELA energy resolution.

served capture yield for each of these resonances and hence they were fitted using the Monte Carlo code TACASI. A good fit to the $J^\pi = 4^-$ s wave at 4.148 keV was obtained using TACASI and the radiative width for this resonance is in good agreement (see Table I) with that reported in BNL-325. The fit to the $J^\pi = 3^-$ resonance at 6.797 keV was not nearly as good, the fitted cross section falling above the data in the higher energy part of the multiple-scattering region. The failure to fit this region is attributed to the effects of resonance-resonance interference with the $J^\pi = 3^-$ resonance at 11.62 keV. TACASI assumes a sum of *non-interfering* (i.e., constructively adding) single-level Briet-Wigner forms for the total and capture cross sections. Hence, the total cross section is overestimated in the region just above the 6.797 keV resonance where the interference reduces the cross section by a factor of approximately 10 [see Garg[7] Fig. 1(a)]. Since the correction for multiple-scatter capture yield involves only the low energy side of the multiple-scattering contribution (where the interference effects are less severe)

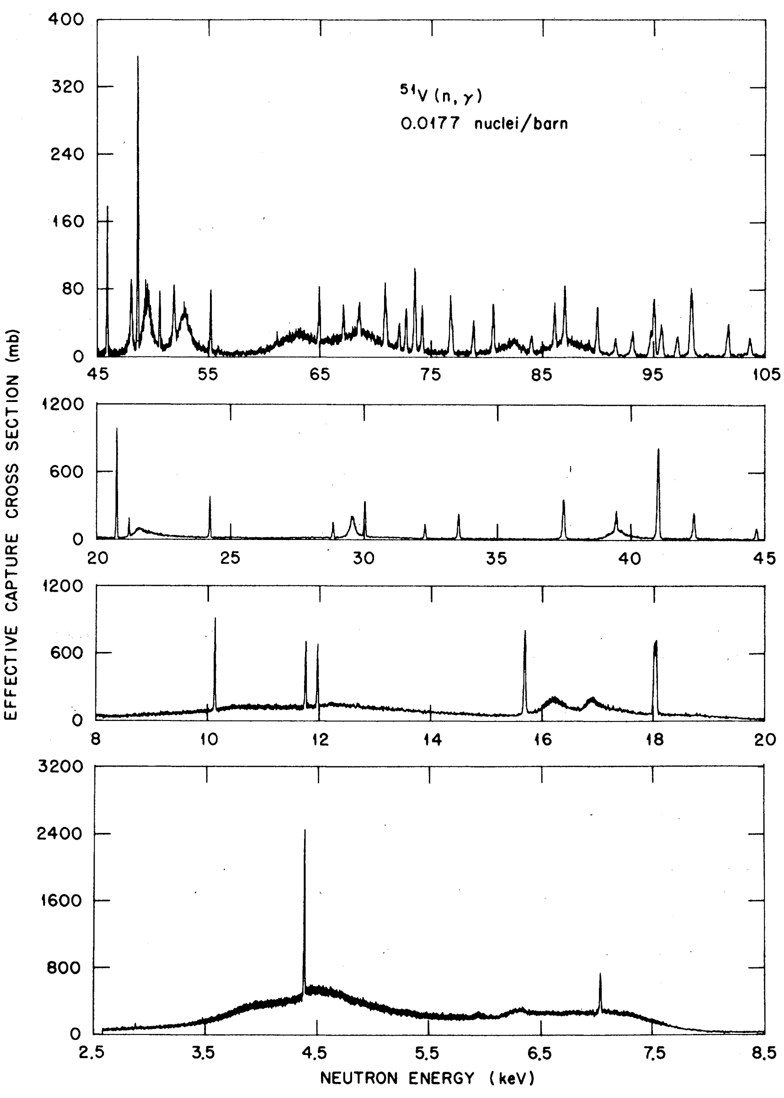

FIG. 3. The $^{51}V(n,\gamma)$ capture cross section from 2.5–105 keV. Note the broad s-wave resonances.

the use of TACASI to fit the 6.797 keV should be approximately valid. The error quoted for the radiative width is derived assuming a 25% uncertainty in the correction for multiple scattering. The value for the radiative width $\Gamma_\gamma = (1.8^{+0.6}_{-0.1})$ eV just overlaps the limits of the value quoted by BNL-325 $\Gamma_\gamma = (2.45 \pm 0.36)$ eV.

TACASI produces a satisfactory fit (Fig. 2) to the 11.62 $J^\pi = 3^-$ resonance, indicating that the resonance-resonance interference effects are not nearly as severe as in the case of the 6.797 keV resonance. This is to be expected since the two resonances are separated by about four full widths of the 6.797 keV resonance. The value for the radiative width derived from the capture data is larger than that listed in BNL-325, however the two values agree within the quoted errors.

There are three narrow p-wave resonances (at 7.031, 11.76, and 11.97 keV) in this region for which the capture kernel $(A_\gamma \equiv g\Gamma_n\Gamma_\gamma/\Gamma_n + \Gamma_\gamma)$ is smaller by a factor of 2 or 3 than that for the average p-wave resonance. If it is assumed that the p-wave radiative widths do not fluctuate by factors as large as 2 from the average, then A_γ measures $g\Gamma_n$ for these resonances. Thus, the capture cross section data yield estimates of these very small neutron widths. The errors quoted in Table I for $g\Gamma_n$ in these cases cover the results obtained using the two spin values $J = 3, 4$.

In Table I are listed the resonance parameters derived from the capture data over this region and, for comparison, the resonance parameters as compiled in BNL-325.[10] The agreement between the two sets of parameters is good. The most notable discrepancies are the doublet at 18 keV reported in BNL-325 as a single p-wave resonance and the values for radiative width for the s-wave resonance at 39.44 keV. In the latter case, there is a narrow, previously unreported resonance at nearly the same energy as the s wave (see Fig. 3), possibly compromising the earlier measurements.

45-105 keV

The only serious discrepancies between the resonance parameters (see Table II) derived from the present work and those given in BNL-325, are for the two broad s-wave resonances at 68.5 and 87.29 keV. In both cases (see Fig. 3), two or more narrow resonances are superimposed on the s wave. The areas of these previously unreported narrow resonances may have been included in the earlier work, thus accounting for the larger values for $g\Gamma_n$ given in BNL-325.

Two of the three broadest s-wave resonance have large (>3.5 eV) radiative widths. However, since one (at 87.29 keV) of these three has a radiative width less than that found for the much more narrow 52.79 keV s wave, the large radiative widths in this region are not correlated with the neutron widths.

The capture kernels A_γ for the 61.11 keV and the 91.55 keV resonances are significantly smaller than the average area for the narrow resonances. As was discussed in the previous section, it can be argued that in such cases A_γ measures $g\Gamma_n$ rather than Γ_γ.

Tentative J assignments (enclosed by parentheses in Table II) have been made for four resonances between 91 keV and 104 keV. Such assignments are based on the quality of the fits (and the data) obtained using various values of J and often are uncertain because the capture cross section shape is relatively insensitive to J (for a high-spin target such as ^{51}V).

105-131 keV

As shown in Figs. 4 and 5, this region features a number of narrow resonances, superimposed on a nearly Gaussian-shaped envelope. It is likely that there is not sufficient information in the envelope to allow a unique decomposition into individual broad resonances. However, as shown in Table III, by using the resonance energies, neutron widths and spins from the total cross section measurements, a decomposition can be found. For this particular decomposition (which is characterized by the minimum value of χ^2_ν), the agreement with Morgenstern[8] does not appear as good as with Garg.[7] This is somewhat misleading, because the large resonance near 118 keV dominates the region, and in fact the resonance energy can be shifted from 118.7 keV to 117.5 keV (Morgenstern's value) with only a modest degradation of the fit (an 18% increase in the value of χ^2_ν). The resonance parameters for the broad s waves resulting from the analysis of this region are subject to large uncertainties and should be treated as nothing more than a parametrization of the cross section data.

The statistical fluctuations of the data account for some of this troublesome uncertainty, but there is strong theoretical justification for doubting that the single-level analysis used in the present work should be applied to this region. The spacing between resonances of a given J^π is comparable to or less than the widths of some of the resonances. Hence, resonance-resonance interference effects in the capture[18,19] as well as in the scattering cross section may be important. In that case the use of the single-level Breit-Wigner resonance form is not justified. It would be interest-

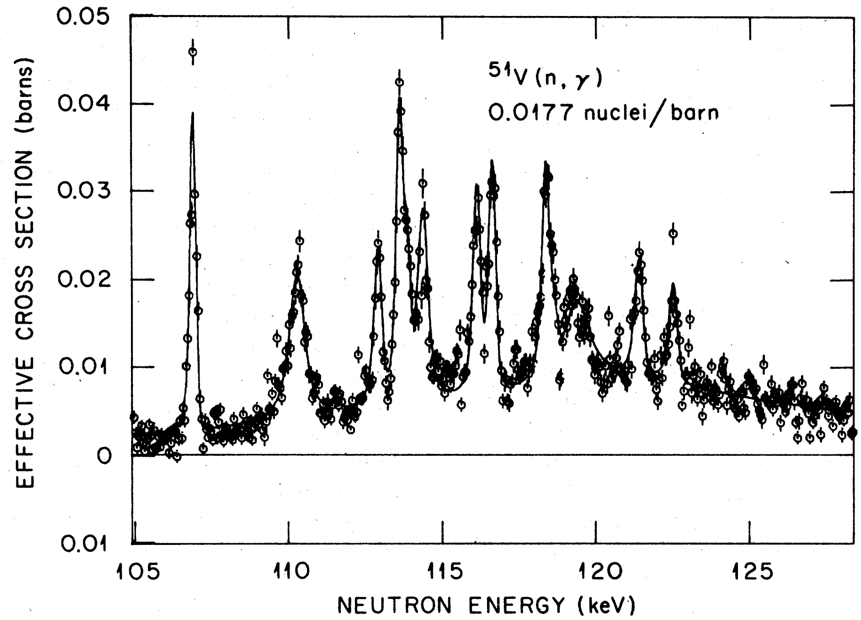

FIG. 4. Capture data and fit for the region 105–128 keV incident neutron energy. The solid curve is the fit to the data obtained by the LSFIT least squares code.

ing to examine the partial radiative widths from these overlapping resonances for interference effects.[20]

Note that the doublet at 129.17 and 130.70 keV is unresolved by Garg, but is resolved by Morgenstern. The widths derived from the capture data for these two resonances agree well with those reported by Morgenstern. The $J=4$ assignment reported by Garg for a resonance at 129.4 keV is adopted for the 129.17 keV resonance seen in capture. A $J=4$ assignment for the 130.70 keV resonance yields a better fit to the data than for $J=3$, and hence a tentative $J=4$ assignment is made for that resonance.

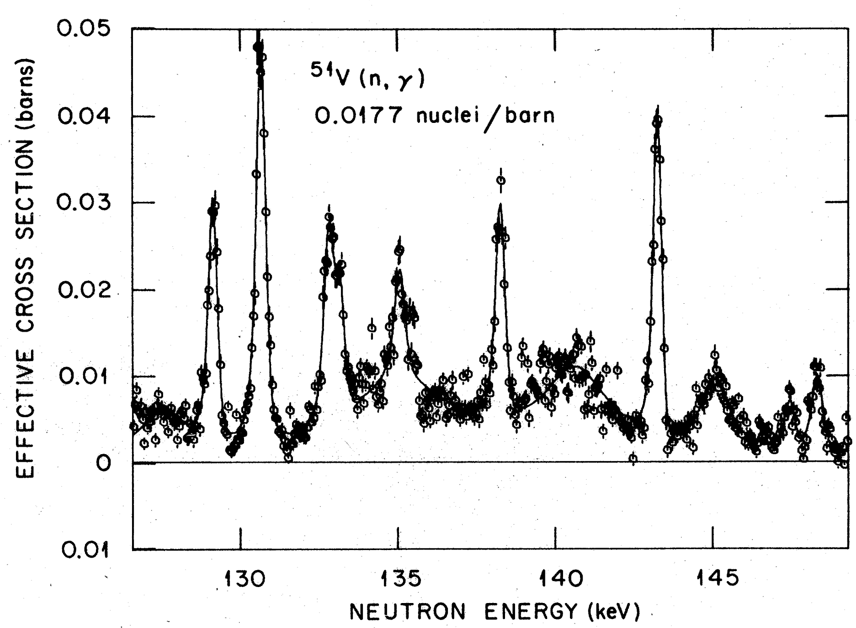

FIG. 5. Capture data and LSFIT fit for the region 128–150 keV incident neutron energy.

131-170 keV

Figures 5 and 6 show the data and resulting fits to this region. Here the resonance energies agree well with those reported by Garg,[7] but the widths disagree well outside the quoted errors (see Table IV). The doublets near 135 keV and 160 keV are located at energies at which Garg reports single resonances. Thus, the widths Garg reports for these resonances may be too large because they essentially represent the areas ($g\Gamma_n$) of both unresolved resonances. The situation near 141 keV and 145 keV is more difficult to understand since these resonances are reasonably well separated from other resonances. Since both resonances are 3^- and the spacing (4.7 keV) is approximately twice either width, it would seem unlikely that resonance-resonance interference can be invoked to resolve the discrepancy.

The capture data near 167 keV consists of four narrow resonances superimposed on a broad envelope. A broad s-wave resonance reported by Garg at 166.7 keV fits the envelope well and hence Garg's resonance energy, neutron width, and spin are adopted.

170-192 keV

As is clear from Fig. 7, fluctuations in the capture data (possibly due to the background corrections) and superimposed narrow resonances tend to obscure the very broad s-wave resonances reported by Garg[7] in this region. In order to analyze these data, the resonance energies, spin and parity assignments, and neutron widths for the broad s-wave resonances are taken from Garg's work. Two resonances not reported by Garg are broad enough to allow a determination of the neutron width as well as the radiative width from the capture data.

The broad s-wave resonance reported by Garg at 177 keV apparently has a small radiative width. In fact, the capture cross section (see Fig. 7) shows a valley between resonances at roughly 177 keV. All attempts to fit this region resulted in a value for the radiative width for the 177 keV resonance [after correction for the scattered neutron sensitivity $K(E)$], consistent with zero. The upper limit (see Table IV) placed on the radiative width by the present work is the uncorrected radiative width deriving from the best fit of this region.

192-215 keV

In this region (see Fig. 8), the resonances are well enough defined to allow the determination of total widths (see Table IV) for six resonances. Of these, Garg[7] reports neutron widths for three (194 ± 1, 200 ± 1.5, and 211 ± 1.5 keV). The neutron widths derived from the capture data agree well with Garg's results for the 194 and 201 keV resonances. However, the neutron width reported by Garg for the 211 keV resonance is intermediate in value between the widths of two closely spaced resonances at 210.5 and 212.2 keV seen in capture. These two resonances were analyzed assuming the $J^\pi = 3^-$ assignment reported by Garg for the 210.5

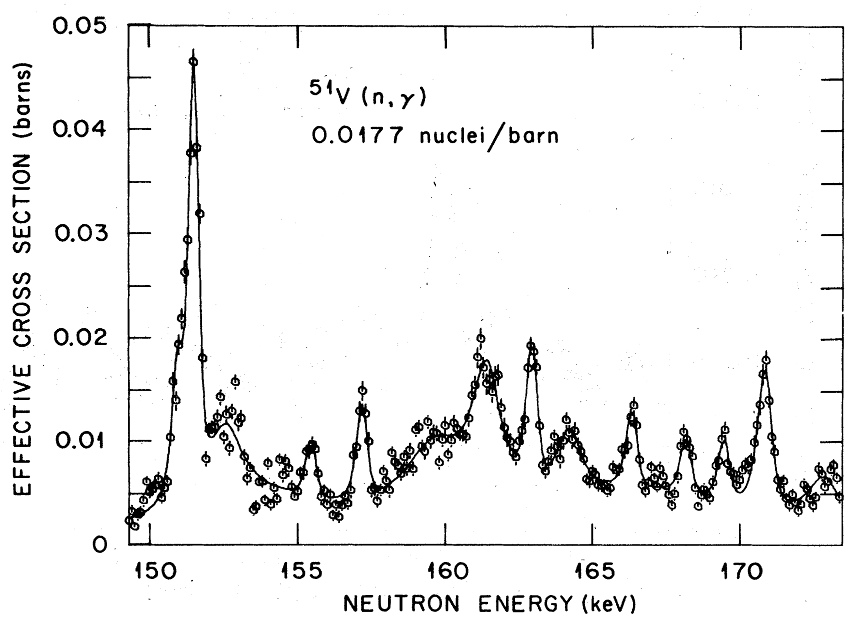

FIG. 6. Capture data and LSFIT fit for the region 150–170 keV.

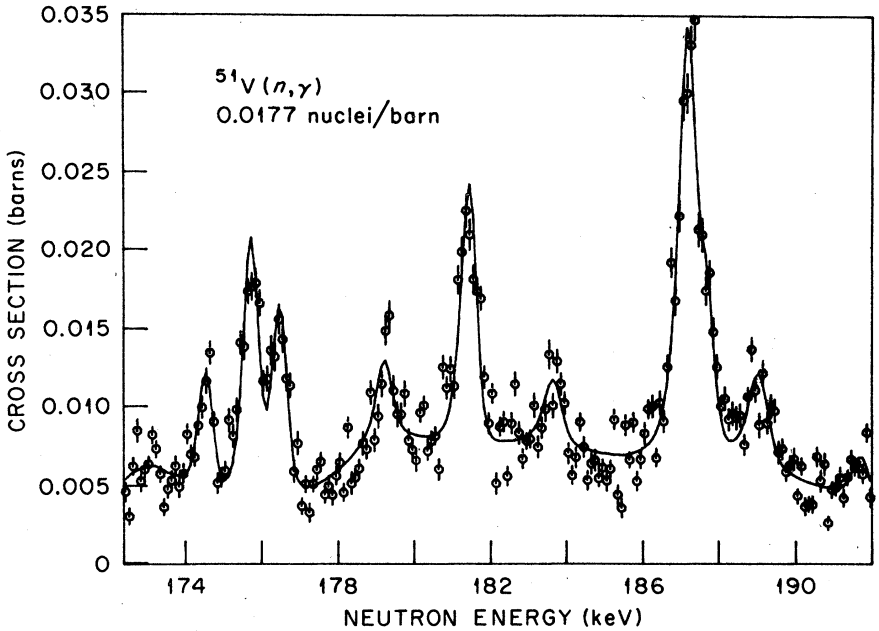

FIG. 7. Capture data and LSFIT fit for the region 170–192 keV. Note the overlapping broad s-wave resonances in this region.

keV resonance. A somewhat better fit for the 212.2 keV results for a $J=3$ assignment than for a $J=4$ and hence a tentative $J=3$ assignment is made for that resonance. Since these two resonances overlap, strong resonance-resonance interference in the neutron channel would be expected if the parity of this resonance is negative. Because the Breit-Wigner single-level formalism used in the present work adequately describes the data, a very tentative positive parity ($l=1$) assignment (indicated by parentheses in Table IV) is suggested for this resonance. Tentative J assign-

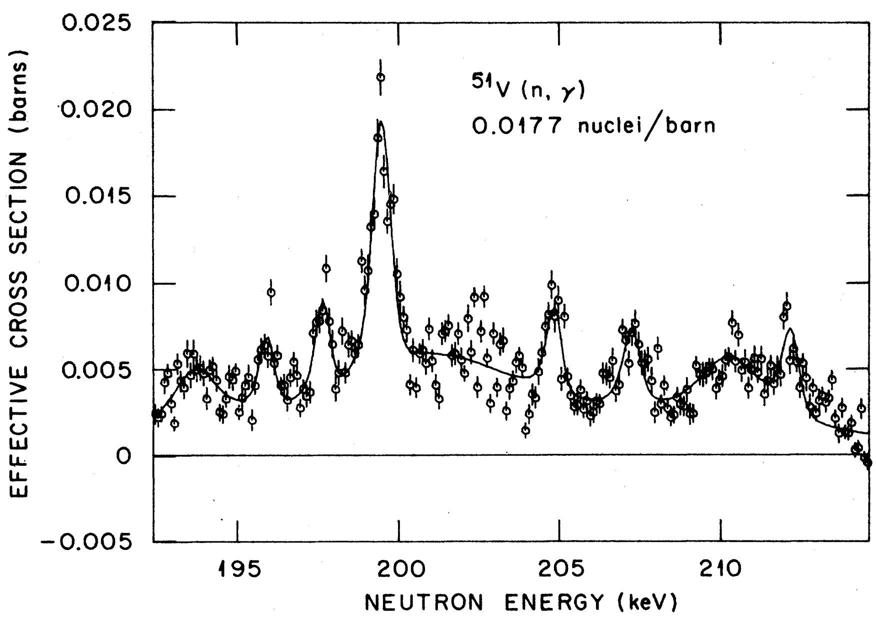

FIG. 8. Capture data and LSFIT fit for the region 192–215 keV.

ments are also made for two other resonances (195.9 and 207.3 keV) in this region. These assignments are based on the quality of the fits obtained for $J = 3, 4$.

ANALYSIS OF RESONANCE PARAMETERS

We analyzed 139 resonances in the $^{51}V(n,\gamma)$ reaction in the incident neutron energy range 2.5–215 keV. Of these, J^π assignments were available from the literature[7,10] for 45 s-wave, $J^\pi = (3,4)^-$, and for 6 p-wave (even parity) resonances. While the paucity of p-wave assignments precludes a statistical analysis, the sample of s-wave resonances is large enough to justify an attempt to draw some conclusions about the s-wave radiative widths, level densities, reduced neutron widths, and strength functions. There are 24 resonances with $J^\pi = 3^-$ and 21 resonances with $J^\pi = 4^-$ (the resonance at 127.0 keV which Garg[7] reports as 4^- is shown to be a doublet in the ORELA capture data and hence is omitted from the set of resonances). The statistical distributions of both sets are discussed below.

s-wave total radiative widths

Figure 9 speaks eloquently of the large fluctuations of the total radiative widths from resonance to resonance. The average 3^- radiation width is 1467 ± 183; the variance consistent with that of a χ_ν^2 distribution with $\nu = 5$ (degrees of freedom). The average 4^- radiative width is 1629 ± 352 meV;

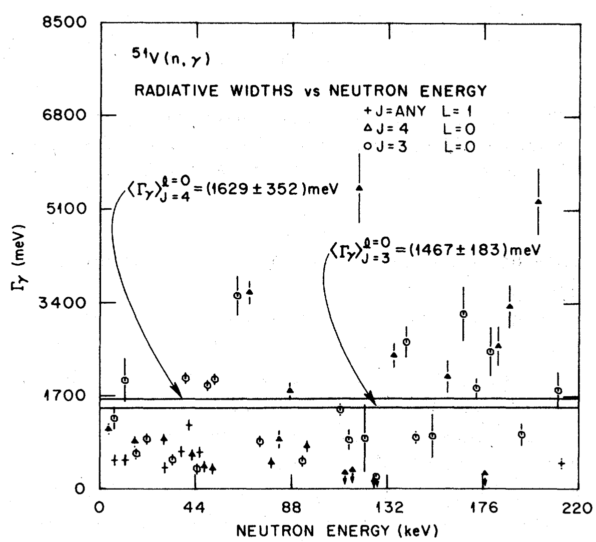

FIG. 9. Total radiative widths in $^{51}V(n,\gamma)$. Note the large fluctuations about the average from resonance to resonance for the s waves. The arrows ↓ indicate upper limits for the radiative widths for the resonances at those energies.

the variance consistent with that of a χ_ν^2 distribution with 2 degrees of freedom. On the basis of a statistical nuclear model[21] the total radiative width is the sum of many partial radiation widths χ^2 distributed with $\nu = 1$, thus, the total radiative width should be described by a χ_ν^2 distribution with a large number of degrees of freedom. The small value of ν for these resonances suggests that the resonances predominately decay to a relatively few lower levels, i.e., the total radiative width is composed of few partial widths. This conjecture is supported by the thermal neutron capture spectrum[22] which shows only six strong primary transitions to within 2 MeV of the ground state of ^{52}V dominating the decay.

The relatively large total radiative widths for these odd parity resonances is consistent with the large widths observed[23] in nuclei neighboring $^{51}V + n$ and the values reported in BNL-325.[10] These large widths are consistent with the conjecture that these resonances are decaying to or near the ground state of ^{52}V by E1 transitions (all low-lying levels of ^{52}V for which J^π assignments are reported[22] are positive parity).

s-wave level spacings

In Figs. 10 and 11 are shown the cumulative number of levels vs energy for each set ($J^\pi = 3^-, 4^-$) of the odd parity resonances. The slopes of these curves yield the observed average level spacings $\overline{D}_J^l$. However, according to Liou and Rainwater,[24] the best estimate to the true level spacing for small to moderately large sample size N is

$$\langle D\rangle_J^l = C_N \overline{D}_J^{\,l}{}^{+\rho_{0.1}^{+}\overline{D}_J^l/N}_{-\rho_{0.1}^{-}\overline{D}_J^l/N} ,$$

where the asymmetrical errors and the coefficient C_N reflect the asymmetric distribution of resonance spacings drawn from an orthogonal ensemble of resonances. The parameters $\rho^\pm$ are here chosen to span the 90%–10% confidence interval.

The $J^\pi = 4^-$ levels (see Fig. 11) can be described well by the mean level spacing $\langle D\rangle_{J=4}^{l=0} = (9.8^{+0.8}_{-0.5})$ keV. In order to determine whether or not the fluctuations about the average spacing are statistically significant, the Dyson and Mehta[25] statistic Δ_3 which is sensitive to misplaced or misassigned levels or deviations from the assumed statistical distributions was calculated. The observed value of $\Delta_3^{\rm obs} = 0.39$ is within the spread of values expected $\Delta_3 = 0.30 \pm 0.11$.

The situation appears somewhat different for the level spacings of the $J^\pi = 3^-$ resonances. As Fig. 10 shows, the level spacings can be well described by two mean values: $\langle D\rangle_{J=3}^{l=0} = (6.1^{+1.1}_{-0.8})$ below 90 keV and $\langle D\rangle_{J=3}^{l=0} = (8.1^{+1.4}_{-1.1})$ keV above 100 keV. Note

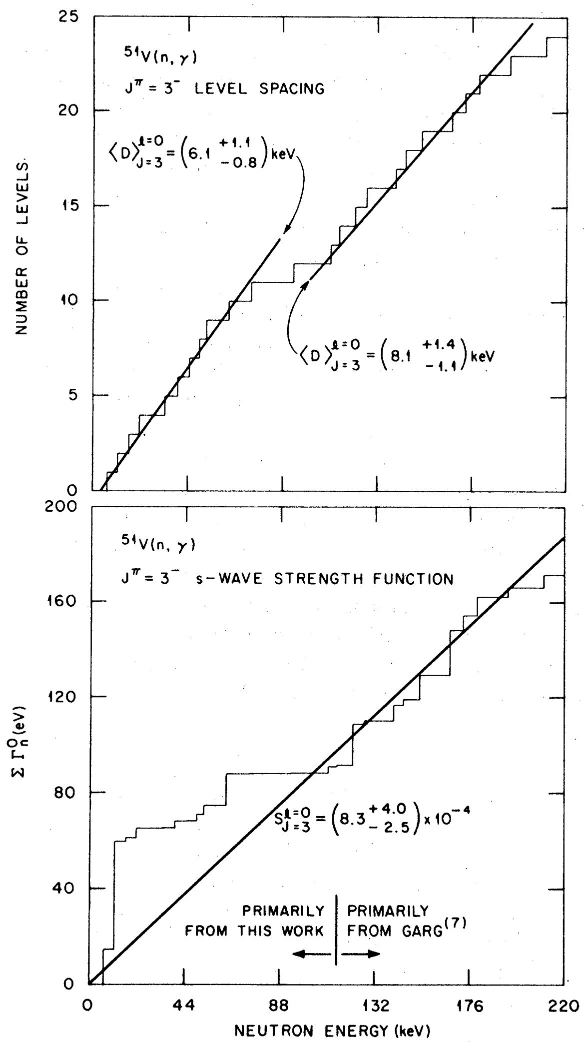

FIG. 10. Level spacing and neutron strength function for the $J^{\pi}=3^{-}$ resonances in $^{51}V(n,\gamma)$. The apparent change in mean level spacing near 100 keV is probably due to missing levels. Assuming three missing small levels (see text), the mean level spacing is $\langle D\rangle^{l=0}_{J=3}$ $=(7.8^{+0.5}_{-1.7})$ keV. For a discussion of the asymmetric errors see test and Ref. 24.

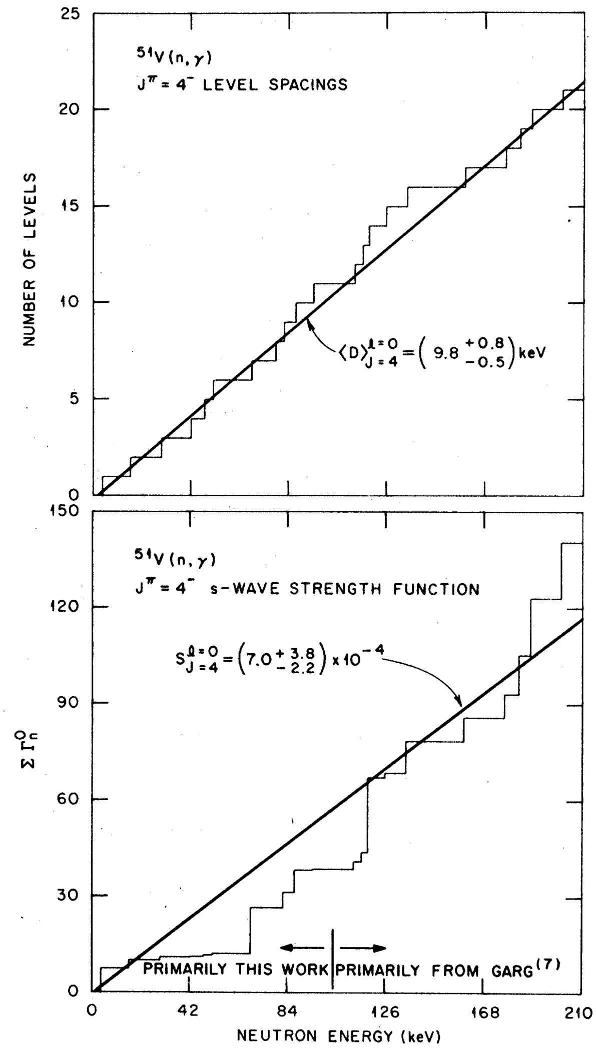

FIG. 11. Level spacing and neutron strength functions for the $J^{\pi}=4^{-}$ resonances in $^{51}V(n,\gamma)$. For a discussion of the asymmetric errors see text and Ref. 24.

that the errors quoted are for the 90–10% confidence interval. The observed value $\Delta_3^{obs}=0.47$ is just outside the range of expected values $\Delta_3=0.32\pm0.11$. Hence, the deviation from a constant slope seems to be attributable to missed and misassigned resonances. As is shown below, the effect is probably due to missing levels. In view of the caution that previous experiments have used in making the J^{π} assignments, it appears unlikely that there could be the three or four misassignments necessary to remove the observed effect. Certainly the Δ_3 test for the $J^{\pi}=4^{-}$ resonances does not indicate that any of those assignments should be $J^{\pi}=3^{-}$.

There are four resonances seen both in the present capture experiment and in Garg's[7] total measurements which could account for missing levels between 90–100 keV. Of these four, tentative J assignments have been made from the capture data (see Table II) for three, at 95.70 keV and 98.4 keV, $J=4$ and at 97.12 keV, $J=3$. However, adding the two $J=4$ resonances to the $J^{\pi}=3^{-}$ set *increases* the discrepancy between the observed and expected Δ_3 statistic.

Fits of the Porter-Thomas distribution to the observed $\{\Gamma^{0}_{n}\}^{l=0}_{J=3}$ distribution are consistent with not more than three missing 3^{-} levels which, if properly located, would remove the apparent change in $\langle D\rangle_{J=3}^{l=0}$. One example (and there may be many others) of such a triad of levels consists of the resonance at 97.12 keV (tentatively assigned as 3) and the two small unassigned resonances at 80.59 and 157.21 keV (see Tables II and III). If these three are *arbitrarily* added to the set of 3^- levels, the Δ_3 statistic takes the value $\Delta_3^{\text{obs}}=0.33$ which is well within the expected range indicating that the $J=3$ assignments are possibly (though not at all likely) correct. Note that this exercise should *not* be construed as an argument for the 3^- assignment for the triad of resonances. The level spacings for this extended set are well described by a single value for the mean spacing $(7.8^{+0.5}_{-0.4})$ keV. This is, of course, precisely the observed 3^- mean level spacing corrected for the expected number of missing levels, hence an adequate description of the 3^- level spacings in terms of a single mean spacing would be $\langle D\rangle_{J=3}^{l=0}=(7.8^{+0.5}_{-1.7})$ keV. Note that the lower error limit has been arbitrarily extended to include the observed mean spacing below 90 keV.

The independent particle model[21] predicts for the level density $\rho=1/\langle D\rangle$, $\rho\propto(2J+1)\exp[-J(J+1)/2\sigma^2]$, where σ^2 is the spin cutoff parameter. After correcting for missing levels, the observed ratio of level densities is

$$\frac{\rho(J^\pi=3^-)}{\rho(J^\pi=4^-)}=1.2\pm0.3\,,$$

where the error limits are obtained by combining the larger error limit for each spacing in quadrature. This result implies a spin cutoff parameter $\sigma^2=9^{+18}_{-3}$.

Reduced neutron widths

The reduced neutron widths Γ_n^l given in the tables of resonance parameters are calculated using reduction factors (proportional to the penetrabilities) appropriate for a square well and a channel radius $a=6.26$ fm, i.e.,

$$s\text{ wave: }\ \Gamma_n^0=\Gamma_n\left(\frac{1\text{ eV}}{E(\text{eV})}\right)^{1/2},$$

$$p\text{ wave: }\ \Gamma_n^1=\Gamma_n\left(\frac{1\text{ eV}}{E(\text{eV})}\right)^{1/2}\left(1+\frac{1}{(ka)^2}\right),$$

where E(eV) is the resonance energy expressed in eV and k is the reciprocal wavelength of the incident neutron. Below 105 keV, neutron widths for most of the s-wave resonances have been determined in the present work. Above 105 keV, in most cases, Garg's[7] neutron widths have been assumed. Because Garg[7] and other workers[8-10] have extensively discussed the reduced neutron width distributions, the discussion here is brief and restricted to the region 2.5–105 keV.

The average reduced neutron width of the $J^\pi=3^-$ resonances is $\langle\Gamma_n^0\rangle=7.76\pm2.6$ eV. The variance of the observed distribution is consistent with that expected for a χ^2 distribution with $\nu\approx0.7$ degrees of freedom. This agrees well with the usual assumption that the reduced neutron widths are Porter-Thomas[26] distributed, i.e., a χ^2 distribution with $\nu=1$.

The three $J^\pi=3^-$ resonances at 6.797, 11.62, and 63.01 keV are noteworthy because they comprise 0.75% of the Wigner single-particle width $\gamma_{sp}{}^2=fh^2/ma^2$. Here $f=2.94$, a factor[27] which describes the reflection of partial waves from the nonphysical square-well potential, is calculated using the approximation suggested by Peaslee.[28] The 11.62 keV resonance alone accounts for 0.46% of $\gamma_{sp}{}^2$.

The average reduced neutron width of the $J^\pi=4^-$ resonances is $\langle\Gamma_n^0\rangle=3.51\pm0.99$ eV, the variance consistent with that of a χ^2 distribution with $\nu=1.2$ degrees of freedom, again in good agreement with the expected Porter-Thomas distribution.

No $J^\pi=4^-$ resonance below 105 keV represents more than 0.15% of the single-particle width and the total fraction is 0.42%.

s-Wave strength functions

Figures 10 and 11 show the cumulative reduced neutron widths over the range of the capture experiment. (Note that above 105 keV, most of the neutron widths are from the work by Garg.[7]) The observed strength function $\overline{S}_J^l$ is defined as $\overline{S}_J^l=\langle\Gamma_n^0\rangle J/\langle D\rangle_J^l$. However, according to Liou and Rainwater,[24] the best estimate of the true strength function based on a moderate sized sample of neutron widths is given by

$$\langle S\rangle_J^l=C_N\overline{S}{}_J^{l}{}^{+\sqrt{2/N'}\overline{S}_J^l\rho^+}_{-\sqrt{2/N'}\overline{S}_J^l\rho^-}\,,$$

where N is the sample size and ρ_-^+ are chosen so as to span the 90%–10% confidence interval. The strength functions derived from Figs. 10 and 11 are $\langle S\rangle_{J=3}^{l=0}=(8.3^{+4.0}_{-2.5})\times10^{-4}$ units and $\langle S\rangle_{J=4}^{l=0}=(7.0^{+3.8}_{-2.2})\times10^{-4}$ units. Both values are in good agreement with the peak in the s-wave strength function predicted by the optical model.[12] The fluctuations in the cumulative sum of Γ_n^0 are consistent with Porter-Thomas fluctuations.

s-WAVE CONTRIBUTION TO THE THERMAL AND 30 keV CAPTURE CROSS SECTION

The capture cross section at thermal neutron energies can be written

$$\sigma_\gamma(E_{TH})=\pi\lambda\!\!\!^{-}(E_{TH})\lambda\!\!\!^{-}(E_i)\sum_{i=1}^{N}\frac{g\Gamma_{ni}\Gamma_{\gamma i}}{E_i{}^2+[\Gamma_i(E_{TH})/2]^2}\,,$$

where $\Gamma_i(E_{TH}) = [\lambda\!\!\!^{-}(E_i)/\lambda\!\!\!^{-}(E_{TH})]\Gamma_{ni} + \Gamma_{\gamma i}$ for a resonance at energy E_i, N is the number of s-wave resonances, and $E_{TH} = 0.0253$ eV. The present work (using many of Garg's values for the neutron widths above 105 keV) yields $\sigma_\gamma(E_{TH}) = 3.95$ b, with the 4.148, 6.797, and 11.62 keV resonances contributing 3.79 b of that total. The preferred value[10] for the thermal capture cross section is 4.88 b. The discrepancy may be due to the presence of one or more bound levels.

For the astrophysical applications it is not the thermal capture cross section which is of interest, but rather the cross section averaged over an ensemble of particles whose kinetic energy is described by a Maxwell-Boltzmann distribution characterized by stellar interior temperatures ~ (2–3) $\times 10^8$ °K, i.e., average particle kinetic energies of the order of 30 keV. The 30 keV Maxwellian-averaged capture cross section derived from this work of (41 ± 3) mb is somewhat larger than the old value recommended by Allen *et al.*[29] of (25 ± 8) mb.

RESONANCE INTEGRAL

The resonance integral can be expressed as a sum over all bound levels above the cadmium cutoff energy ($E_c = 0.5$ eV),

$$I_\gamma \approx 4.09 \times 10^6 \left(\frac{A+1}{A}\right)^2 \sum_i \frac{g_i \Gamma_{ni} \Gamma_{\gamma i}}{E_i^{\,2} \Gamma_i},$$

where $g_i\Gamma_{ni}$, $\Gamma_{\gamma i}$, Γ_i, and E_i have their usual meanings for resonance parameters and taking Garg's values for many of the neutron widths above 105 keV, the capture experiment yields a contribution to the resonance integral of 0.56 b. Dresner[30] shows that the I/v low energy contribution to I_γ is given by $0.45\sigma_\gamma(E_{TH})$. Using $\sigma_\gamma(E_{TH}) = 4.88$ b yields a value $I_\gamma \gtrsim 2.75$ b in agreement with the recommended value[10] of (2.7 ± 0.1) b.

CORRELATION COEFFICIENTS $\rho(\Gamma_n, \Gamma_\gamma)$

Over the past decade or so a good bit of evidence[6] has accumulated showing that assumptions about the statistical behavior of radiative and neutron widths may not be warranted for nuclei near closed shells. In particular, in the cases[31,32] of neutron capture in ^{88}Sr and in ^{90}Zr, large positive correlations between the reduced neutron and radiative widths are reported. Such correlations are predicted by the valency model. In that model the incident neutron excites simple single-particle configurations which then decay by γ emission to final states which are also simple single-particle configurations, and the partial radiative width $\Gamma_{\gamma i}$ is given by[6,33,34]

$$\Gamma_{\gamma i} \propto \Gamma_{ni}^{l}\,\theta_f^2,$$

where Γ_{ni}^{l} is the reduced neutron width of the initial state and θ_f^2 is the reduced width of the final state. If the total radiative width is dominated by one partial width, then it would show the correlation with the reduced neutron width. Table VI summarizes the correlation coefficients $\rho(\Gamma_n^0, \Gamma_\gamma)$ observed for the two sets of s-wave resonances $J^\pi = 3^-, 4^-$.

The column labeled $P_>$ lists the probability of exceeding the observed correlation coefficient as calculated by drawing random samples of reduced widths from a Porter-Thomas distribution and radiative widths from χ_ν^2 distributions where ν is derived from the variance of the radiative widths for the sample being tested. The correlation coefficient for the $J^\pi = 3^-$ resonances is marginally significant when all 24 resonances are included; however, below and above the region 105–128 keV the correlation is less significant. The decrease in significance is due to the reduction in sample size rather than any strong correlation in the excluded region as indicated by the last entries in Table VI for the 3^- resonances. The $J^\pi = 4^-$ resonances show a statistically significant correlation (at the >99.9% confidence level) for various sample compositions: (1) all $J^\pi = 4^-$, (2) only the resonances below 105 keV (for which almost all neutron widths and radiative widths were determined in the capture ex-

TABLE VI. Correlation coefficients for the s-wave resonances in $^{51}V(n,\gamma)$.

	$J^\pi = 3^-$				$J^\pi = 4^-$			
Energy range comments	Sample size	$\rho(\Gamma_n^0, \Gamma_\gamma)$	ν [a]	$P_>$ [b]	Sample size	$\rho(\Gamma_n^0, \Gamma_\gamma)$	ν [a]	$P_>$ [b]
$2.5 \leq E_\lambda \leq 215$ keV	24	0.42	5	3.9%	21	0.93	2	<0.1%
$E_\lambda < 105$ keV	12	0.43	4	9.0	11	0.92	3	<0.1
$E_\lambda > 128$ keV	8	0.65	9	6.2	6	0.84	5	2.1
$E_\lambda < 105$ keV or $E_\lambda > 128$ keV	20	0.43	6	4.0	17	0.90	3	<0.1

[a] Number of degrees of freedom implied by variance analysis of resonances in sample.
[b] Probability of exceeding the observed $\rho(\Gamma_n^0, \Gamma_\gamma)$ randomly drawing reduced neutron widths from a Porter-Thomas distribution and the radiative widths from a χ_ν^2 distribution.

periment), and (3) a sample excluding the resonances in the range 102–128 keV (the region in which there is considerable discrepancy among the various sets of resonance parameters discussed above). The highest energy sample consisting of all 4^- resonances above 128 keV yields a slightly less significant correlation coefficient (98% confidence level).

In order to demonstrate that the observed $(\Gamma_n^0, \Gamma_\gamma)$ correlation for the 4^- resonances does not reflect a gross underestimate of the scattered-neutron sensitivity, the correlation coefficients were also calculated using as radiation widths values equal to the lower bounds set by the errors listed in the Tables I–IV. These errors are larger than the correction for scattered neutron sensitivity. The correlation coefficients so calculated remain significant at >99.7% confidence level, except for the sample of six resonances above 138 keV (see Table VI). In the latter case, the correlation is still significant at the 90% confidence level.

The observation of large correlations between the reduced neutron widths and total radiative widths is consistent with the prediction by Bird *et al.*[6] that valency effects should be significant near mass 50. A more detailed comparison of the partial radiative widths and the predictions of the valency model is called for but requires greater information about the final states and partial widths than is presently available. In particular, the γ ray energy resolution of the TED's is not sufficient to distinguish the low lying excited states of ^{52}V. Also, the spin and parity assignments of those levels should be better determined before a detailed comparison is attempted.

CONCLUSIONS

The resonance parameters and associated statistics (level spacings, strength functions, average radiative and reduced neutron widths, and resonance contribution to the thermal cross section are expected to at least partially answer the need for better known cross sections for vanadium in conjunction with its use as a structural material in fusion processes.

The analysis of the resonance parameters has shown "nonstatistical" effects in the radiative width distributions ($J^\pi = 3^-, 4^-$). The significant correlation between the reduced neutron widths and total radiative widths reported here is consistent with the prediction by Bird *et al.*[6] that the valency model of neutron capture should be important near the closed shell at mass 50. More detailed comparisons with the valency model require more nearly complete knowledge of the partial widths and final states than is presently available.

ACKNOWLEDGMENTS

One of the authors (R. R. W.) is grateful for the support which ERDA has provided throughout this work. The authors are very appreciative of R. Spencer's help in using the Monte Carlo code TACASI and to G. de Saussure for his help in the calculations of the Dyson-Metha Δ_3 statistic.

[1]D. Steiner, Nucl. Fusion 14, 33 (1974).
[2]D. I. Garber and R. R. Kinsey, BNL Report No. BNL-325, 3rd edition 11, 1976 (unpublished).
[3]P. Genther *et al.*, Report No. ANL/NDM-24, 1977 (unpublished).
[4]J. B. McGrory, Phys. Rev. 160, 915 (1967).
[5]H. Horie and K. Ogawa, Prog. Theor. Phys. 46, 439 (1971).
[6]J. R. Bird *et al.*, Proceedings ICINN, Lowell, Mass., 1976 (unpublished).
[7]J. B. Garg, Nucl. Sci. Eng., 65, 76 (1978).
[8]J. Morgenstern *et al.*, Nucl. Phys. A123, 561 (1969).
[9]R. G. Stieglitz, R. W. Hockenbury, anx R. C. Block, Nucl. Phys. A163, 592 (1971).
[10]S. F. Mughabghab and D. I. Garber, BNL Report No. BNL-325, 3rd edition 1, 1973 (unpublished).
[11]R. L. Macklin and B. J. Allen, Nucl. Instrum. Methods 91, 565 (1971).
[12]R. L. Macklin, N. W. Hill, and B. J. Allen, Nucl. Instrum. Methods 96, 509 (1971).
[13]B. J. Allen, A. R. de L. Musgrove, R. L. Macklin, and R. R. Winters (unpublished).
[14]B. J. Allen and R. L. Macklin, Phys. Rev. C 3, 1737 (1971).
[15]R. L. Macklin, Nucl. Sci. Eng. 59, 12 (1976); Report No. ORNL-TM-4810 (unpublished).
[16]F. H. Fröhner, General Atomic Report No. GA-6906, 1966 (unpublished).
[17]R. R. Spencer, private communication.
[18]E. P. Wigner, Phys. Rev. 70, 606 (1946).
[19]A. M. Lane and R. G. Thomas, Rev. Mod. Phys. 30, 257 (1958).
[20]R. E. Coté and L. M. Bollinger, Phys. Rev. Lett. 6, 695 (1961).
[21]J. E. Lynn, *The Theory of Neutron Resonance Reactions* (Clarendon Press, Oxford, 1968).
[22]R. L. Auble, Nucl. Data Sheets, 25, No. 2 (1978).
[23]For example, see Ref. 10, Fig. 4, p. xxiii.
[24]H. I. Liou and J. Rainwater, Phys. Rev. C 6, 435 (1972).

[25]F. J. Dyson and M. L. Mehta, J. Math. Phys. 4, 701 (1963).
[26]C. E. Porter and R. G. Thomas, Phys. Rev. 104, 483 (1956).
[27]G. Michand, L. Scherk, and E. Vogt, Phys. Rev. C 1, 864 (1970).
[28]D. C. Peaslee, Nucl. Phys. 3, 255 (1957).
[29]B. J. Allen, J. H. Gibbons, and R. L. Macklin, *Advances in Nuclear Physics*, edited by M. Baranger and E. Vogt (Plenum, New York, 1971), Vol. IV.
[30]L. Dresner, *Resonance Absorption in Nuclear Reactions* (Pergamon Press, New York, 1960).
[31]J. W. Boldeman, B. J. Allen, A. R. de L. Musgrove, R. L. Macklin, and R. R. Winters, Nucl. Phys. A269, 397 (1976).
[32]J. W. Boldeman, B. J. Allen, A. R. de L. Musgrove, and R. L. Macklin, Nucl. Phys. A246, 1 (1975).
[33]A. M. Lane and S. F. Mughabghab, Phys. Rev. A 240, 445 (1975).
[34]J. Cugnon, Nucl. Phys. A263, 61 (1976).